Effect of Massive Neutrino on Large Scale Structures

P. R. Dhungel, S. K. Sharma and U. Khanal
Central Department of Physics,
Tribhuvan University, Kirtipur, Nepal

January 4, 2012

Abstract

Jeans mass calculated with different combination of parameters involved has shown interesting variation with remarkable shifting of position of peak value from x = m/T = 0.5 to 5.5. The standard deviation is 2.217. In particular, using the harmonic mean square velocity, shifts the peak Jeans mass to x = m/T $\sim$ 2, which is remarkably less than previously reported value of 4.2. Different scales of neutrino structures including virialized moments have also been compared.

1 Introduction

The enigmatic neutrino has generated great deal of interest in cosmology for a long time. Regarding the number of neutrino species e.g., calculation of primordial nuclear abundances in cosmology had arrived at the number of neutrino species $N_\nu < 4$ [1] long before it was experimentally established at CERN[2]; the current value is $N^\nu = 2.994 \pm 0.013$ [3]. Similar calculations set the baryon to photon ratio at $\sim 4.7 \times 10^{-10}$, which in turn has determined the present baryon density in the Universe to be $\Omega_B h^2 = 0.0223$, where $\Omega_B = \rho_B/\rho_c$ is the present baryon density in units of the critical density, and h is the present value of the Hubble parameter in units of $100\, km/s/Mpc$, that is expected to be $h \sim 0.72(3)$[4]. Writing the present neutrino density

as $\Omega_\nu h^2 = m_{eV}/31$, where m_{eV} is the average rest-mass of the three species neutrino in eV, it is easily seen that the $31\,eV$ neutrino will close the Universe; this closure mass is referred to as the Cowsik-McClelland bound[5], although in their paper they had used a smaller value of Ω and four component neutrino to arrive at $8\,eV$. Tremain and Gunn [6] set the limit that a neutrino of $m_\nu < 1MeV$ cannot reside in the halo of galaxy to contribute significantly to the dark matter. Bond et al [7] calculated the maximum Jeans mass for structures of neutrino to be $M_{\nu m} \approx 1.2 \times 10^{17} m_{eV}^{-2} M_\odot$, where m_{eV} is the neutrino mass in eV.

As recent results show that the mass difference between neutrino species is very slight, $\Delta m^2 \sim 10^{-5}\,eV^2$, in this paper, we consider three neutrino species of similar mass. Comparing the baryon and neutrino densities, we see that even a $0.7\,eV$ neutrino will have dominated over baryon by now. Rather than whether the neutrino is massive, the question at present is how massive it is; again cosmology provides the most stringent limit $\sum m_\nu < 0.6\,eV$ [11, 12]. So the neutrino appears as a very important component of the Universe. Consequently, it should have a strong bearing on structure formation. It decouples at very early times, and then evolves as a totally independent component that interacts only gravitationally. Indeed the filamentary structures, sheets, walls and voids as exposed by various surveys point towards dissipationless collapse of clouds of particles like neutrinos into Zeldovich pancakes[13] at some stage of evolution. Although the cosmological neutrino has been studied extensively, we feel that our analysis gives some further insight on structure formation, particularly at what temperature the structures are more likely to form and spectrum of the size / mass of the structures at various temperatures.

The momentum of a freely moving particle in the Friedmann-Robertson-Walker spacetime is redshifted by the expansion, i.e., the comoving momentum $pa = y$ remains constant, where p is the momentum and a the scale factor. Using $v = p/E$ for the velocity and the Einstein energy-momentum relation, $a^2E^2 = p^2a^2 + m^2a^2 = y^2 + x^2$, we see that Eva remains constant during expansion, and as the number density scales as a^{-3}, $\rho v a^4$ also remains constant where ρ is the density. As the light neutrinos decouple at the very high temperature of $T \approx 1MeV$ while still extremely relativistic (ER), they are essentially in free fall since then. So their number density is always distributed as

$$dn = \frac{g}{2\pi^2}\left(\frac{m}{x}\right)^3 \frac{y^2}{e^y+1}dy \tag{1}$$

where g is the number of spin degeneracy (six, for the three $\nu - \overline{\nu}$ pairs), and we have used the fact that $T \sim 1/a$; Planck units in which $G = c = k_B = \hbar = 1$ are used throughout this work. As $E \sim p >> m$ in the extreme relativistic (ER) regime, Eq.(1) represents the Fermi-Dirac distribution. In the non-relativistic (NR) case however, $E \sim p^2/2m + m$, and Eq. (1) is no more a Fermi-Dirac distribution.

Integrating dn over y from 0 to ∞ gives the number density $n = \frac{g}{2\pi^2}\Gamma(3)\eta(3)\left(\frac{m}{x}\right)^3$ where Γ and η are the gamma and eta functions respectively[15]; also, $\eta(n) = (1 - 2^{1-n})\,\zeta(n)$. Thus we can write down the expectation value of any regular function as $< f(y) >= \frac{1}{\Gamma(3)\eta(3)}\int_0^\infty dy \frac{y^2}{e^y+1} f(y)$.

The width of the momentum distribution shown in Fig. 1 is characterized by $y_{max} = 3.131$ where the distribution is maximum. Some other characteristic values that we will use are the mean $y_{mean} =< y >= \frac{\Gamma(4)\eta(4)}{\Gamma(3)\eta(3)} = \frac{7\zeta(4)}{2\zeta(3)} = 3.151$, the root-mean square $y_{rms} =< y^2 >^{1/2}= \sqrt{\frac{15\zeta(5)}{\zeta(3)}} = 3.597$,the harmonic mean $y_{hm} =< y^{-1} >^{-1}= \frac{3\zeta(3)}{\zeta(2)} = 2.192$, and the root harmonic mean square $y_{rhms} =< y^{-2} >^{-1/2}= \sqrt{\frac{\Gamma(3)\eta(3)}{\Gamma(1)\eta(1)}} = \sqrt{\frac{3\zeta(3)}{2\ln(2)}} = 1.613$ are also useful to describe the width of the distribution.

The particle speed is $v = p/E = y/\sqrt{y^2 + x^2}$. In the ER case as $y >> x$, $v(y) \to 1 - \frac{x^2}{2y^2} + ...$ giving $v_{mean} \to 1 - \frac{1}{2}\left(\frac{x}{y_{rhms}}\right)^2 \to v_{rhms}$; also, $v_{hm} =< 1/v >^{-1} \to 1 - \frac{1}{2}\left(\frac{x}{y_{rhms}}\right)^2 \to v_{rhms}$. Three averages of v are shown in Fig. 2. Thus, we see that v_{rhms} is the more representative speed in the ER regime. These ideas can be used for a bosonic system as well by replacing η with ζ . But $\zeta(1) = \infty$, so $v_{rhms}(boson) = 0$, indicative of the liability of bosons to condense into a zero momentum state. Although a zero momentum state is strictly forbidden for a fermionic system, as $\eta\,(1) = \ln\,(2)$, a low momentum condensate characterized by the harmonic mean values is possible. The rms energy is given by $a^2E_{rms}^2 = y_{rms}^2 + x^2$, and another characteristic value of the energy is the velocity averaged momentum $a^2E_v^2 =< y^2 >< 1/v^2 >= y_{rms}^2(1 + x^2/y_{rmhs}^2)$. Obviously, as $a \to 0$, $E \to \infty$.

Any macroscopic quantity that depends on the momentum distribution will be sensitive to the averaging process. This will be even more so in the

relativistic regime. In this paper, we look into such effects and investigate the possible distribution of the sizes of neutrino structures. In particular, we would like to determine whether smaller neutrino structures could have formed in the very early Universe. In the next Section, we apply these ideas to the gravitating neutrino spheres, and compare the distributions of Keplerian, Virial and Jeans and the free streaming scales.

2 Neutrino Jeans Mass

The Jeans mass that is contained within the Jeans radius, $M_J = \frac{4\pi R_J^3 \rho_\nu}{3} = \frac{1}{2}(\frac{R_J^3}{R_\nu^2})$, has the momentum dependence [14],

$$\frac{M_J}{C} = \frac{x^2 y^3}{(y^2 + x^2)^{7/4}}, \tag{2}$$

where the constant $C = \frac{\pi^{7/2} m_{Pl}^3}{6\sqrt{g\eta(3)m^2}} = \frac{1}{m_{eV}^2\sqrt{g}} \times 15 \times 10^{18} M_\odot$, m_{Pl} is the Planck mass, x = ma = m/T and y = pa = p/T . Any gas cloud of radius greater than R_J will contain a mass greater than M_J, in which case gravitation can overcome the free streaming motion of the neutrinos to produce a collapse. This analysis can be used for any or all the components of the Universe, and here we will apply it to the neutrino. These characteristic length and mass scales, being dependent on the momentum distribution, are sensitive to the averaging process.

J.R. Bond *et al*[7] calculated M_J by comparing the pressure and the density as $< M_J >_1 \sim \langle \rho v^2 \rangle^{3/2} / \langle \rho \rangle^2$, which was found to peak at $x_1 = 4.2$. This expression may be appropriate in the gravitational collapse of a mass of a gas against its internal pressure, but the neutrinos are free-streaming since decoupling. Thinking that k_J is the fundamental quantity that determines the Jeans scale, we calculated $< M_J >_2 \sim \langle \rho v^2 \rangle^{3/2} / \langle k_J \rangle^3$ and found the peak to be at $x_1 = 2.5$. We can also find the average of the Jeans mass as $< M_J >_3 = < M_J(y) >$ with peak at 5.0, and represent some characteristic values analytically by $< M_J >_4 = < M_J(y_{rms}) >$ with peak at 4.2, and $< M_J >_5 = < M_J(y_{rhms}) >$ with peak at 1.9. Plot of these values are displayed in Fig. 3. The values of x at which these M_J's peak are given in the table 1. The results show quite a wide variations in the Jeans mass ranging across a magnitude. Also the time when these structures can form, determined by

Table 1: The value x_p at which the different means of neutrino Jeans mass peak and also the peak value. As the maximum of the x_p's is 5, the different $< M_J >$'s are caculated at this value and the standard deviation is determined.

Method	x_p	$M_J(x_p)$	$M_J(x=5)$	Standard Deviation
$< M_J >_1$	4.2	1.75	1.71	
$< M_J >_2$	2.1	0.73	0.36	
$< M_J >_3$	5.0	1.61	1.61	0.832
$< M_J >_4$	4.2	2.06	2.01	
$< M_J >_5$	1.9	0.41	0.21	

x, varies from 1.9 to 5. In essence two groups of neutrino structures could appear: the smaller one at $x \sim 2$ when the neutrino are still quite relativistic with $v_{rhms} \sim 0.6$, and the ten times larger one at $x \sim 5$ when the neutrinos have become non-relativistic with $v_{rhms} \sim 0.3$.

3 Neutrino structure scales

To investigate the scales of neutrino structures, let us rewrite the Friedmann equation in terms of the Hubble radius $R_H = 1/H$ in the following form,

$$\frac{R_{H_0}^2}{R_H^2} = \frac{H^2}{H_0^2} = \frac{R_{H_0}^2}{\xi^2}\left(\frac{d\xi}{dt}\right) = \frac{\rho}{\rho_{c0}} + \frac{1-\Omega}{\xi^2} = \frac{f(\xi)}{\xi^4}. \tag{3}$$

Here the subscript 0 represents the respective values at some reference time t_0 and $\rho_c = \frac{3H^2}{8\pi}$ is the critical density; ρ is the total energy density contributed by matter and radiation, while $1-\Omega$ may be considered to be the energy density due to curvature, and in particular, $f(\xi) = \Omega_{\Lambda 0}\xi^4 + (1-\Omega_0)\xi^2 + \Omega_{d0}\xi + \Omega_{\gamma 0} + \Omega_{\nu rest0}\sqrt{(\xi^2 + (y/x_0))}$ ...., where $\xi = x/x_0 = a/a_0 = T_0/T, \Omega_{\Lambda,d,\gamma,\nu}$ are the respective contributions to the total density at t_0 (in units of critical density) by the cosmological constant, pressureless dust, photon, neutrino, etc. In the way we have written the neutrino density, we need not make the distinction between radiation and matter domination as its density scales appropriately in the respective regime

$$\rho_\nu/\rho_{c0} \to \begin{cases} \Omega_{\nu 0}/\xi^4, & \xi \to 0, \quad (ER) \\ \Omega_{\nu\, rest\, 0}/\xi^3, & \xi \to 0, \quad (NR). \end{cases}$$

The ratio of neutrino and photon density is

$$\frac{\Omega_\nu}{\Omega_\gamma} = \frac{\rho_\nu}{\rho_\gamma} = \left(\frac{T_\nu}{T_\gamma}\right)^4 \frac{3\zeta(3)}{4\zeta(4)} x\langle\sqrt{1+(y/x)^2}\rangle = \frac{\Omega_{\nu.rest}}{\Omega_\gamma}\langle\sqrt{1+(y/x)^2}\rangle. \quad (4)$$

The temperature ratio T_ν/T_γ is unity at very high temperature and is $(4/11)^{1/3}$ at temperatures below the neutrino decoupling and $e^+ - e^-$ annihilation, i.e., $T_\nu < 1MeV$; the density ratio rises linearly in the NR region. The temperature of photon-neutrino equality can be determined by setting Eq. ((4)) equal to unity, whence one finds $x_{eq} = 3.179$.

The most important length scale in cosmological context is the Hubble radius; the ratio of the comoving Hubble radii at equality and at arbitrary time is given by

$$\left(\frac{R_{H_{eq}}/a_0}{R_H/a}\right)^2 = \left(\frac{\xi R_{H_{eq}}}{R_H}\right)^2 = \frac{f_\nu(\xi)}{\xi^2}. \quad (5)$$

A length scale relevant to a gravitationally bound gaseous system is the radius where the escape speed becomes equal to the average random speed of the gas particles viz., $v^2 = 2M/R_{esc} = \frac{8\pi}{3}\rho R_{esc}^2$, or $\frac{1}{R_{esc}^2} = \frac{8\pi\rho}{3v^2}$. As the smooth background of photons will not contribute to the potential well, $\rho = \rho_\nu$. We can use the expression for critical density to write the ratio of the comoving Hubble and escape radii in a suggestive form that looks similar to Eq. (5):

$$\left(\frac{\xi R_{H_0}}{R_{esc}}\right)^2 = \frac{f_{esc}(\xi)}{\xi^2}, \quad (6)$$

where

$$f_{esc}(\xi) = \Omega_{\nu rest0}\langle\sqrt{\xi^2 + (y/x_0)^2}\rangle/v^2. \quad (7)$$

We can also define the Keplerian radius R_K by $\frac{1}{R_K^2} = \frac{4\pi\rho}{3v_{rot}^2} = \frac{1}{2R_{esc}^2}$ with the understanding that v stands for the rotational speed; obviously, any particle orbiting with $v_{rot} > v_{esc}$ will escape. Similarly, the virial radius given by $2 < v^2 >= M < 1/R_V >$ leads to $\frac{1}{R_V^2} = \frac{4\pi\rho}{6v^2} = \frac{1}{4R_{esc}^2}$. Another such scale, the Jeans radius is given by $\frac{1}{R_J^2} = \frac{4\rho}{\pi v^2} = \frac{3}{2\pi^2 R_{esc}^2}$. All these length scales are some numerical multiples of R_{esc}.

In any spectral analysis, it is the wavenumber $k \sim 1/R$ that is fundamental, and similarly, in the Jeans analysis, the Jeans wavenumber k_J should

be averaged over all momenta. We have seen that R_{esc} is the underlying quantity, so let us look into the behaviour of $1/R_{esc}^2$. There are a number of ways of averaging Eq. (6), as discussed in the previous section:

$$\left(\frac{\xi R_{H_0}}{R_{esc}}\right)^2_1 = \frac{\Omega_{\nu\, rest\, 0}}{\xi^2}\left\langle \frac{(\xi^2+(y/x_0)^2)^{3/2}}{(y/x_0)^2}\right\rangle \quad \texttt{from} \left\langle\frac{\rho}{v^2}\right\rangle \tag{8a}$$

$$\left(\frac{\xi R_{H_0}}{R_{esc}}\right)^2_2 = \frac{\Omega_{\nu\, rest\, 0}}{\xi^2}\left\langle \sqrt{\xi^2+(y/x_0)^2}\right\rangle\left\langle \frac{\xi^2+(y/x_0)^2}{(y/x_0)^2}\right\rangle \texttt{from}\langle\rho\rangle\left\langle\frac{1}{v^2}\right\rangle \tag{8b}$$

$$\left(\frac{\xi R_{H_0}}{R_{esc}}\right)^2_3 = \frac{\Omega_{\nu\, rest\, 0}}{\xi^2}\frac{\langle\sqrt{\xi^2+(y/x_0)^2}\rangle^2}{\langle(y/x_0)^2/\sqrt{\xi^2+(y/x_0)^2}\rangle} \quad \texttt{from}\ \frac{\langle\rho\rangle}{3P} \tag{8c}$$

where, in the last sub-equation, P stands for pressure and v^2 has been replaced by $3P/\rho$. The plot of R_{esc} averaged in three ways of Eq. (8) are displayed in Fig. 6 for a flat universe, but the general trend for closed and open is also the same:R_{esc} increases to a maximum value, and then decreases slowly with the expansion of the universe. But there are drastic differences in the values of the last average relative to the first two; e.g., for $\Omega_{\gamma\, eq} = \Omega_{\nu\, eq} = 0.5$ that is shown, we find that the maximum of $\left(\frac{R_{esc}}{\xi R_{H_0}}\right)_{1max} = 0.757$ occurs at $\xi = 0.847$, that of $\left(\frac{R_{esc}}{\xi R_{H_0}}\right)_{2max} = 0.477$ occurs at $\xi = 0.922$, and $\left(\frac{R_{esc}}{\xi R_{H_0}}\right)_{3max} = 1.074$ at $\xi = 1.632$. These different values indicate a spectrum of possible length scales. We may combine Eqs. 5 and 6 to write

$$\frac{R_H}{R_{esc}} = \sqrt{\frac{f_{esc}(\xi)}{f_\nu(\xi)}} \tag{9}$$

This relation, displayed in Fig 5, shows that the horizon crossing at $R_H/R_{esc} = 1$ occurs at different times for different averages. R_J, proportional to R_{esc}, will also show similar behaviour.

The smallest of all these length scales, R_{esc}, enters the horizon the earliest, while the largest, R_J, enters later. It appears that the time lag between R_J entering horizon at the onset of Jeans instabilities, the virialization of the cosmic neutrino inside a smaller R_V that entered the horizon earlier, and even the Keplerization of the gas in an even smaller length R_K cannot be great.

We can also calculate the netrino mass within R_{esc} viz., $M_{esc} = \frac{4\pi}{3}\rho_\nu R_{esc}^3$ that simplifies to $\frac{M_{esc}}{R_{H_0}} = \frac{(y/x_0)^3\xi^2}{\sqrt{\Omega_{\nu\,rest\,0}}(\xi^2+(y/x_0)^2)^{7/4}}$. Here also, as in the previous section, the averaging over the momentum of M_{esc} can be done in many different ways. Below, we give three which we think are useful:

$$\left\langle \frac{M_{esc}}{R_{H_0}} \right\rangle_1 = \frac{0.5}{\sqrt{\Omega_{\nu\,rest\,0}}} \left\langle \frac{(y/x_0)^3\xi^2}{(\xi^2+(y/x_0)^2)^{7/4}} \right\rangle \tag{10}$$

$$\left\langle \frac{M_{esc}}{R_{H_0}} \right\rangle_2 = \frac{0.5}{\sqrt{\Omega_{\nu\,rest\,0}}} \left\langle \frac{(y/x_0)^2}{\xi^2+(y/x_0)^2} \right\rangle \left\langle \frac{(y/x_0)\xi^2}{(\xi^2+(y/x_0)^2)^{3/4}} \right\rangle^{1/2} \tag{11}$$

$$\left\langle \frac{M_{esc}}{R_{H_0}} \right\rangle_3 = \frac{0.5}{\sqrt{\Omega_{\nu\,rest\,0}}} \left\langle \frac{\xi^2+(y/x_0)^2}{(y/x_0)^2} \right\rangle^{-1} \left\langle \frac{(y/x_0)\xi^2}{(\xi^2+(y/x_0)^2)^{3/4}} \right\rangle^{1/2} \tag{12}$$

A plot of (M_{esc}/R_{H_0}) is shown in Fig. 4 for three different averages. Although the nature of the curves are same, the peaks are seen to occur at different positions.

4 Virial Equation and Moments

Moments of the virialized quantities have played very important role in revealing the features of large astrophysical objects. Some of these methods are used here to describe the large scale neutrino structures that should be the precursors of the galactic and the supercluster scales. The formation of large-scale structures proceeds with the gravitational collapse of clouds of matter composed of baryons, cold dark matter and hot dark matter whose major constituent is the neutrino. Much work has been done to investigate the evolution of size and eccentricity of spherical and spheroidal / ellipsoidal clusters [8, 9, 10], and and also the relavant masses. In the majority of these works, Virial theorems / equations and their moments of various orders have been used. In this section, various moments of the Jeans mass are calculated using using the ideas of Virial moments. The results are compared with the values presented in the previous section.

In a system of N particles, gravitational forces tend to pull the system together and the stellar velocities tend to make it fly apart. It is possible to relate kinetic and potential energy of a system through the change of its

moment of inertia. In a steady-state system, these tendencies are balanced, which is expressed quantitatively through the Virial Theorem. A system that is not in balance will tend to move towards its virialized state. The Scalar Virial Theorem tells us that the average kinetic and potential energy must be in balance. The tensor Virial Theorem tells us that the kinetic and potential energy must be in balance in each separate direction. The scalar Virial Theorem is useful for estimating global average properties, such as total mass, escape velocity and relaxation time, while the tensor Virial Theorem is useful for relating shapes of systems to their kinematics, e.g. the flatness of elliptical galaxies to their rotational speed.

The Virial Equations of the various orders are, in fact, no more than the moments of the relevant hydrodynamical equations. The scalar Virial Equation for a system is given by

$$\frac{1}{2}\frac{d^2I}{dt^2} = 2K + U \tag{13}$$

where the moment of inertia about the origin $I = \frac{1}{2}\int \rho r^2 dV$, the kinetic energy is $K = \frac{1}{2}\frac{d^2}{dt^2}\int_V \rho v^2 dV$ and the potential energy is $U = \frac{\rho_c}{2}\int_V \frac{\rho}{r} dV$, where $\rho_c$is the core density. Thus the Virial Equation of the 1st order is given by

$$\frac{1}{2}\frac{d^2}{dt^2}\int_V \rho r^2 dV = \frac{1}{2}\frac{d^2}{dt^2}\int_V \rho v^2 dV + \frac{\rho_c}{2}\int_V \frac{\rho}{r} dV \tag{14}$$

The Virial Equation of the 2nd order is given by just multiplying the integrand by r before integrating:

$$\frac{1}{2}\frac{d^2}{dt^2}\int_V \rho r^3 dV = \frac{1}{2}\frac{d^2}{dt^2}\int_V \rho v^2 r dV + \frac{\rho_c}{2}\int_V \rho dV \tag{15}$$

Similarly, the higher order equation may be written. For the steady state, 2K + U = 0. This gives the virial radius of the spherical cluster:

$$R_V^2 = \frac{3}{4\pi}\left(\frac{v^2}{\rho}\right) \tag{16}$$

Writing ρ and v in terms of x = ma = m/T and y = pa = p/T, as discussed in Introduction section, we have

$$R_V = Constant. \frac{y}{(y^2+x^2)^{7/4}} \left(\frac{x}{m}\right)^2 \tag{17}$$

and hence the expectation value of this virial radius is given by

$$< R_V >= Constant. \int_0^\infty dy \frac{y^3}{(e^y+1)(y^2+x^2)^{7/4}} \left(\frac{x}{m}\right)^2 \tag{18}$$

Its evolution has been shown in 7.

The Virial Mass of the cluster contained within this radius may be calculated as $< M_V >= constant. < R_V >^3 < \rho >$. Its variation with x is as expected (9), but peaks at x = 3.73 in contrast to the position of peaks of Jeans masses calculated in section 2, where the peaks have occurred at x = 1.9, 2.1, 4.2 and 5.0. [14, 7]

4.1 Virial moments of Jeans mass

As stated earlier, in the virial method, we take the moments of the equation of motion. These equations obviously involve the moments of the distribution of density, pressure, velocity, gravitational potential, etc. Here we are taking the spatial moments of various orders of Jeans mass given by 2: The 1st moment of Jeans mass is given by

$$\begin{aligned} \langle M_J R_V \rangle &= constant. \int_0^\infty dy \frac{y^2}{(e^y+1)} (M_J R_V) \\ &= Constant. \int_0^\infty dy \frac{y^6 x^4}{(e^y+1)(y^2+x^2)^{5/2}} \end{aligned} \tag{19}$$

The 2nd and 3rd moments may be written in similar fashion. The variations of the 1st, 2nd and 3rd moments with x have been shown in 8.The 1st and the 2nd are found to peak and at x = 12.2 and 27.02 respectively, but the 3rd moment appears to plateau off from x ~ 100 to large values of x. Jeans masses may be calculated by dividing these moments by $< R_V >$, $< R_V^2 >$ and $< R_V^3 >$ respectively. The variation of these masses with x has been shown in 9 (For comparison $< M_J >$ and $< M_V >$ have also been

Table 2: Temperatures at which the peaks of the Jeans masses occur for different neutrino masses.

M_J from	x for M_J peaks	Temp. (K) corresponding to x for		
		m_ν= 1 eV	m_ν= 0.2 eV	m_ν= 0.01 eV
$\frac{\langle \rho v^2 \rangle}{\langle \rho \rangle^2}$	1.9	6100	1220	61
$\frac{\langle \rho \rangle}{\langle K_J \rangle^3}$	2.1	5519	1104	55
$< R_V >^3 < \rho >$	3.73	3107	621	31
$M_J(y_{rms})$	4.2	2760	552	28
$\langle M_J(y) \rangle$	5	2318	464	23
1st moment of M_J	6.48	1789	358	18
2nd moment of M_J	8.01	1447	289	14
3rd moment of M_J	9.58	1210	242	12

plotted). They have peaked at x = 6.48, 8.01 and 9.58. Following table gives the corresponding temperatures at which the peaks of the Jeans masses occur for a few typical neutrino masses:

From the above analysis, it is seen that the large-scale structures of neutrinos of different mass and random velocity distribution can form at different neutrino temperatures, corresponding to different time. The earliest peak that occurs at x = 1.9 corresponds to the time when the neutrino temperature was 1220 K for the 0.2 eV neutrino. Similarly, the latest peak occurs at x = 9.58 corresponding to a temperature of 242 K. In between these two values, it is found that the Jeans mass peaks at a number of different x. Thus it can be interpreted to mean that a distribution of neutrino structures of different masses and of different ages should be in existence. Typical masses of these structures range from 6×10^{19} to $4.5 \times 10^{20} M_\odot$.

5 Free Streaming

It is well known that free streaming of collisionless particles wipe out any structures that form. In this context, there are other two scales that are relevant. The first is the particle horizon R_P occurring at the distance to which light would travel since the big bang. The comoving particle horizon

can be written as

$$\frac{R_P}{\xi R_{H_{eq}}} = \int_0^{\xi} \frac{d\xi'}{\sqrt{f_\nu(\xi')}}. \tag{20}$$

No massive particle can cover a distance larger than this. The other is the freestreaming length R_F, the distance a particle travels since the big bang; it is given by an expression similar to Eq. (20), but including the particle speed v inside the integral:

$$\frac{R_F}{\xi R_{H_{eq}}} = \int_0^{\xi} \frac{v d\xi'}{\sqrt{f_\nu(\xi')}} \tag{21}$$

$$= \frac{(\frac{y}{x_{eq}})}{\sqrt{1-\Omega_{eq}}} \int_{y/x_{eq}}^{\sqrt{\xi^2+(y/x_{eq})^2}} \frac{dz}{\sqrt{\left(z^2-(\frac{y}{x_{eq}})^2\right)\left(z^2+\frac{\Omega_{\nu\, rest\, eq}}{1-\Omega_{eq}}z+\frac{\Omega_{\gamma\, eq}}{1-\Omega_{eq}}-\frac{\Omega_{\nu\, rest\, eq}}{1-\Omega_{eq}}\right)}}$$

Any scale that is smaller than R_F will be wiped out by free streaming. The integral Eq. (21) in our case, for different values of $\Omega_{\gamma\, eq}$, can be written as Jacobian elliptic functions [16]

$$\left(\frac{R_F}{\xi R_{H_0}}\right)_{flat} = CF(\phi/k) \tag{22}$$

Considering the flat case where $\Omega_{\gamma\, eq} = 0.5$, the solution is $C^2 = \frac{8(y/x_{eq})^2}{1+\frac{3\zeta(3)}{4\zeta(4)}\frac{y}{x_{eq}}\left(\frac{T_\nu}{T_\gamma}\right)^4}$, $\sin^2\phi = \frac{\sqrt{x_{eq}^2+y^2}-y}{\sqrt{x_{eq}^2+y^2}+y}$, and $k^2 = \frac{\sqrt{x_{eq}^2+y^2}-x_{eq}}{\sqrt{x_{eq}^2+y^2}+x_{eq}}$. A plot of $(R_F/\xi R_{H_{eq}})_{flat}$ is shown in Fig. - 10 for three different mean values of y. This free streaming length is seen to saturate to the values of 4.193, 3.899 and 2.555 as $x \to \infty$, when evaluated with y_{rms}, y_{mean} and y_{rhms} respectively.

For non-flat universe, $R_F/\xi R_{H_{eq}}$ is given by Eqs. (21) and (22) with $C^2 = \frac{(y/x_{eq})^2}{\Omega_{\gamma\, eq}}\sqrt{1+(y/x_{eq})^2}$, $\tan^2(\phi/2) = \sqrt{\frac{(\sqrt{x_{eq}^2+y^2}-y)}{(\sqrt{x_{eq}^2+y^2}+y)}}\frac{(\sqrt{x_{eq}^2+y^2}-y)}{(\sqrt{x_{eq}^2+y^2}+y)}$ and $2k^2 = 1 + (y/x_{eq})^2\left(\frac{1-\Omega_{eq}}{\Omega_{eq}}\right)\sqrt{1+(y/x_{eq})^2}$. Plots of $R_F/\xi R_{H_{eq}}$ for $\Omega_{\gamma\, eq} = 0.45$, are found to saturate to 2.883, 2.113 and 1.690, for the three means of y; and in the closed universe of $\Omega_{\gamma\, eq} = 0.55$, the free streaming length saturates to 2.683, 1.908 and 1.495 for the respective means of y. The nature of the curves are similar to that of flat ones.

6 Discussion and conclusion

From above analysis, it is seen that the large-scale structures of neutrinos of different mass and random velocity distribution can form at different neutrino temperatures, corresponding to different time. The earliest peak that occurs at x = 1.9 corresponds to the time when the neutrino temperature was 1220 K for the 0.2 eV neutrino. Similarly, the latest peak occurs at x = 9.58 corresponding to a temperature of 242 K. In between these two values, it is found that the Jeans mass peaks at a number of different x and hence it can be interpreted to mean that a distribution of neutrino structures of different masses and of different ages should be in existence. Typical masses of these structures range from 6×10^{19} *to* $4.5 \times 10^{20} M_{\odot}$. These are in the order of very large super-clusters which formed first in the hot dark matter scenario. But we should note that as the Universe cools down, and x becomes large, the scale of these structures will come down because the leading term in the Jeans mass, Eq. (2) goes as $x^{-1/2}$. Thus for 1 eV neutrino at the present temperature of 1.96 K ($\sim 10^{-4} eV$), the Jeans mass comes down to the galactic scale. Accordingly, the large superclusters that formed initially would have fragmented to the galactic size.

Thus the massive neutrino can play a very important role in the formation of structures. These particles decouple from the rest of matter at a very early time when the temperature was 1 MeV. Since then they have been cooling down independently without interacting with other matter except gravitation. So the evolution of this component can be considered to occur separately. We have done the Jeans analysis taking into account only neutrino. The results show the possibility of different sizes of neutrino structures forming at different time. In particular, two distinct sizes make their appearance: the smaller ones which could form at relatively higher temperature of $T \sim m/2$ when the neutrinos were still relativistic, and the ten time bigger ones that form when $T \sim m/5$. As these neutrino structures have a mass of order of m_{pl}^3/m^2, these are indeed very large, in the scale of large superclusters. The Jeans mass at lower temperature is of the order of galaxy. In this work we have considered the neutrino as a totally independent component of the Universe that interacts with nothing except gravitation with each other. In reality, these neutrino interact gravitationally with the rest of the matter. So in any volume, there is more matter than just neutrino that is trying to bring about a gravitational collapse. Hence the actual scale at which the neutrino could begin to collapse should be smaller than the value we have derived.

References

[1] Steigman, G, Schramm, D.N. and Gunn, J.E., Phys. Lett. **66B**, 202 (1977).

[2] Winter, K. (Ed.), *Neutrino Physics*, (Cambridge University Press, 2000), p. 197.

[3] Yao, W.M., *et al*, J. Phys. **G33**, 1 (2006).

[4] Nakamura, K., *et al.* (Particle Data Group), *J. Phys.* ***G*** **37**, 075021 (2010).

[5] Cowsik, R. and McClelland, J., *Phys. Rev. Lett.* **29**, 669 (1972).

[6] Tremaine, S. and Gunn J. E., *Phys. Rev. Lett.* **42**, 407 (1979).

[7] Bond, J.R., Efstathiou, G. and Silk, J., *Phys. Rev. Lett.* **45**, 1980 (1980).

[8] S. Chandrasekhar, *Ellipsoidal Figures of Equilibrium*, 1969, Yale University Press.

[9] S. Chandrasekhar and D. D. Elbert, *MNRAS*, **155**, 435 (1972).

[10] G. Som Sunder and R. K. Kochhar, *MNRAS*, **213**, 381 (1985).

[11] Spergel, D.N., *et. al.*, arxiv: astro-ph/0603449.

[12] Komatsu, E., *et. al.*, arxiv: 1001.4538v3[astro-ph.CO]

[13] Zeldovich, Y.B.,Eiviasto, J. and Shandarin, S.F., *Nature*, **300**, 407 (1982).

[14] Dhungel, P.R.,Sharma, S.K. and Khanal, U., *Scientific World* **2**, 8 (2004).

[15] Abramowitz, M and Stegun, I.A., *Handbook of Mathematical Functions*, (Dover, New York, 1976).

[16] Byrd, P.F. and Friedman, M. D., *Handbook of Elliptic Integrals for Engineers and Scientists*, (Springer, Berlin, 1971).

[17] Gradshteyn, I.S. and Ryzhik, I.M., *Tables of Integrals, Seires, and Products*, 5th ed. (Academic, Boston, 1993).

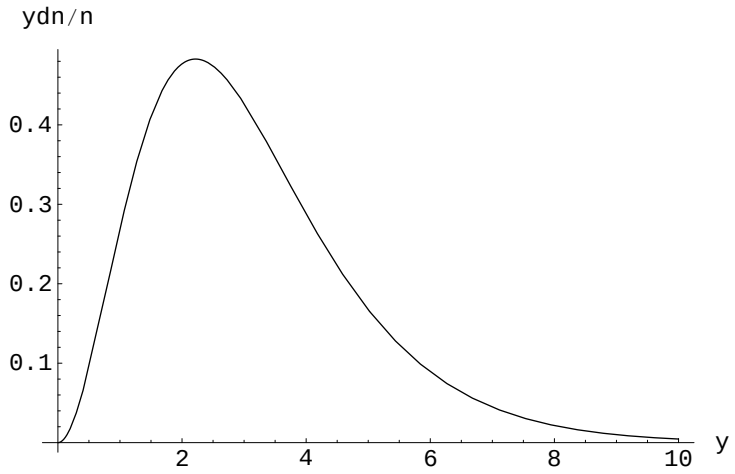

Figure 1: Momentum distribution of the free cosmic neutrino as a function of $y = pa = p/T_\nu$. The distribution is maximum at y_{max} 3.131, and other characteristic values are $y_{rms} =< y^2 >^{1/2}= 3.597$ and $y_{rhms} =< 1/y^2 >^{-1/2}= 1.613$. Such momentum distribution give rise to a spectrum of neutrino structure scales.

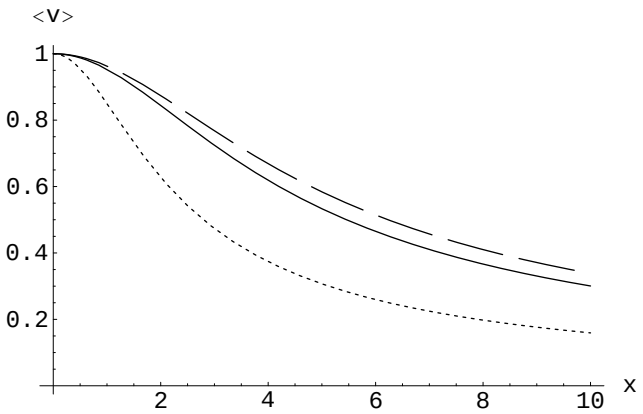

Figure 2: The average speed of the massive neutrino as a function of x. The solid curve is v_{mean}, the dashed curve is v_{rms} and the dotted curve is v_{rhms}. In the extreme relativistic regime as $x \to 0$, it is seen that $v_{mean} \to v_{rhms}$; towards the non-relativistic end it is closer to v_{rms}.

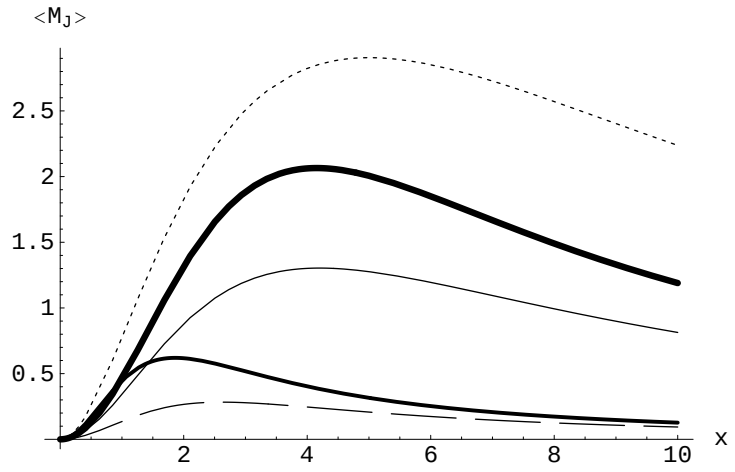

Figure 3: The distribution of Jeans Mass. The dashed curve represents the value calculated by Bond, *et al*, i.e., $< M_J >_1$ The dotted curve is $< M_J >_2$, the thick solid curve is $< M_J >_3$, moderately thick curve is $< M_J >_4$ and the normal curve is $< M_J >_5$. Two distinct groups of Jeans mass are seen, one that peaks at $x \sim 4$ to a value of ~ 4, and another that peaks at $x \sim 2$ to little less than 1. The first group appears to be related to the rms speed and the second to the rhms speed. As pointed out in the text, at the relativistic regime it is the rhms speed that is more representative. So the smaller second group of structures can start to form with smaller mass at earlier times.

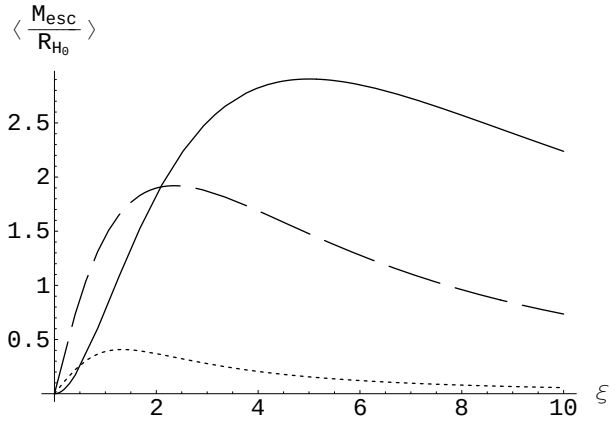

Figure 4: The distribution of Mass contained within escape radius calculated by different averaging process given in equations 10, 11 and 12.The dashed curve represents the value calculated by the 1st equation, the dotted is that of 2nd equation and normal curve is from the third one.

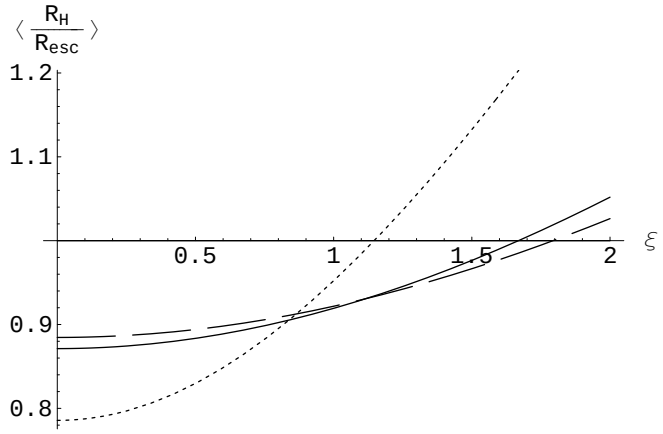

Figure 5: The ratio of R_H/R_{esc} for the three averages.The third average enters the horizon the latest.

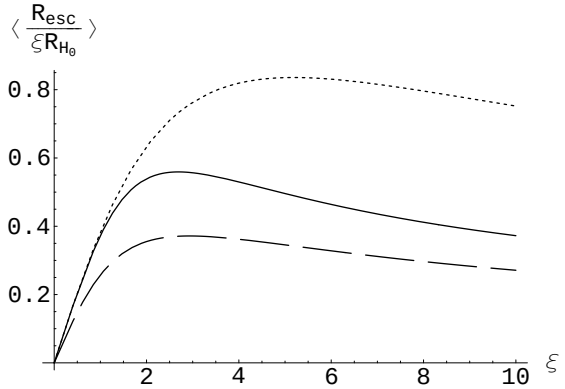

Figure 6: The ratio of $R_{esc}/\xi R_H$ for the three averages.

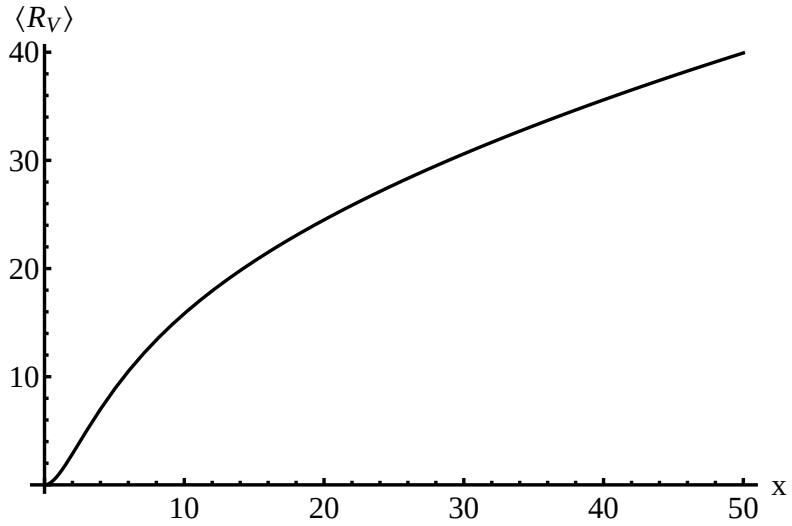

Figure 7: Evolution of Virial Radius $< R_V >$ of a cluster.

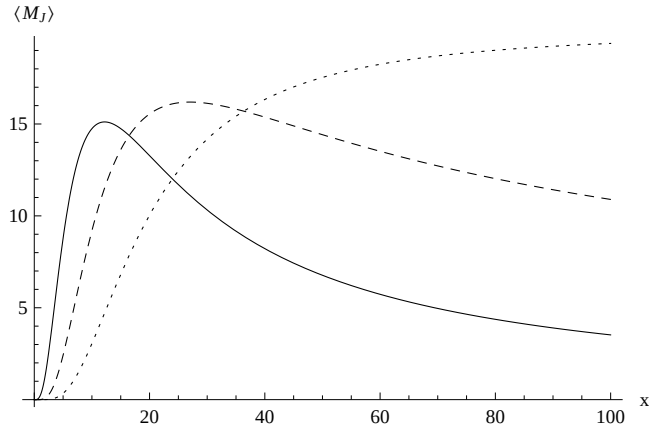

Figure 8: Virialized moments of the first three orders of Jeans masses. The first moment peaks at x ~ m_ν / T = 6.48. The second moment peaks at x = 8.01 and the 3rd one at 9.58.The solid, dashed and dotted lines are for 1st, 2nd and 3rd order moments respectively. They are appropriately scaled to make of equal heights for the comparision purpose.

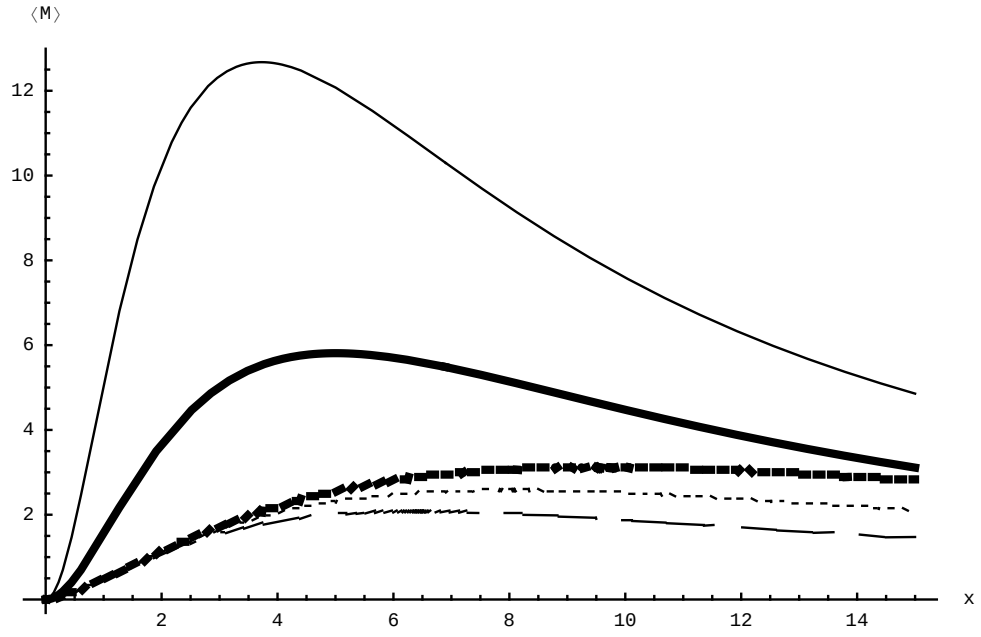

Figure 9: The average cluster masses (Jeans and Virial) against x. The normal curve is for virial mass, thick continuous curve for Jeans mass, the normal dashed curve for the Jeans mass calculated from the 1st moment of the mass and normal dotted and thick dotted are those from 2nd and 3rd moments respectively.

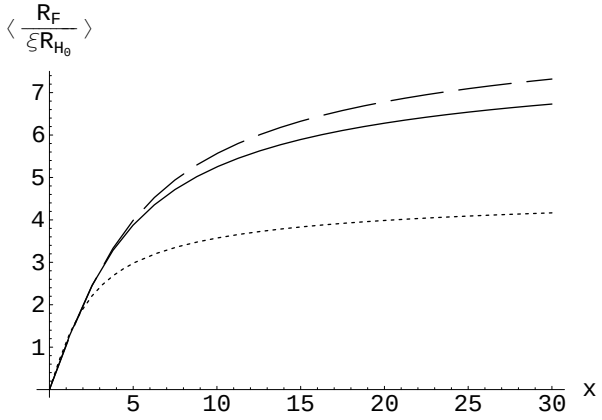

Figure 10: The ratio of $R_F/\xi R_{H_0}$ for the three averages for the flat case.